Ab initio LCAO hybrid density-functional method for accurate, large-scale electronic structure simulations of semiconductor materials, interfaces and gate stacks

Petr A. Khomyakov, Jess Wellendorff, Mattias Palsgaard, Tue Gunst, Haruhide Miyagi, Brecht Verstichel, Fabiano Corsetti, Vaida Arcisauskaite, Umberto Martinez, Anders Blom, and Søren Smidstrup
Synopsys QuantumATK, Copenhagen, Denmark
Email: quantumatk@synopsys.com

***Abstract*—We demonstrate an efficient method for high-accuracy *ab initio* simulations for semiconductor device technology development, such as high-k metal gate stack engineering and investigation of 2D material-based FET performance. The method combines the HSE06 hybrid density functional with linear combination of atomic orbitals (LCAO) basis sets, as implemented in the QuantumATK atomic-scale modeling platform. We show that HSE06-LCAO predicts accurate band energies and enables large-scale HSE06 simulations for systems comprising thousands of atoms using modest computational resources.**

Keywords—DFT, hybrid functionals, HSE06-NEGF, band gaps, band alignment, defects, effective work function, HKMG, 2D-FET

I. Introduction

As the future brings continued down-scaling of semiconductor device technology, computational screening for alternative materials with improved electronic properties, and investigating the impact of defects, dopants and material thicknesses with atomistic simulations, have become a crucial step in developing next-generation advanced logic, memory, power electronics, and quantum computing [1-5]. Recent studies in industry [2,4,5] show that nonlocal HSE06 [6] density functional theory (DFT) simulations are superior for accurate modeling of the band structure of gap materials, band alignment at interfaces, and defect (or dopant) properties, overcoming many limitations of local and semilocal density functionals. However, because of the high computational cost of HSE06 simulations with plane-wave (PW) basis sets (HSE06-PW), this method has so far been practical only for systems with a relatively small number of atoms, limiting the applicability to a small subset of technologically relevant problems [4,5]. We here present an *ab initio* hybrid density functional (HSE06) method with LCAO basis sets [6,7], implemented in the QuantumATK software package by Synopsys® [8,9], along with other hybrid functionals, such as PBE0, B3LYP, and B3LYP5. The HSE06-LCAO method provides both accurate and computationally efficient calculations of band energies, defect trap levels, band offsets, and band diagrams for semiconductor materials, interfaces and stacks comprised of several thousands of atoms. Moreover, the use of LCAO basis sets can be orders of magnitude faster than standard HSE06-PW implementations, enabling simulations for large systems with relatively modest hardware.

II. Simulation Method

The QuantumATK HSE06-LCAO method is based on the approach by Levchenko *et al.* [7]. We introduce an auxiliary basis set to evaluate 4-center integrals using a resolution of the identity approach, and use the pair-atom resolution of the identity (PARI) approximation, which allows us to achieve linear scaling for HSE06-LCAO simulations with respect to system size, N, whereas HSE06-PW simulations scale as $O(N^3\log(N))$. We use norm-conserving pseudopotentials of two different kinds; FHI with single-zeta-polarized (SZP) or double-zeta-polarized (DZP) basis sets, and PseudoDojo (PD) with "Medium" or "High" basis sets, as implemented in QuantumATK [8,9]. HSE06-PW simulations have also been done using projector-augmented wave (PAW) potentials.

III. Results and Discussion

A. Band gaps of bulk materials

Electronic structure calculations for 30 gap materials (including Si, SiO_2, HfO_2, SiC, InAs, GaN, MoS_2, and others) in Fig. 1 show that HSE06-LCAO provides high quality of results (QOR) for band energies, as expected for HSE06, which

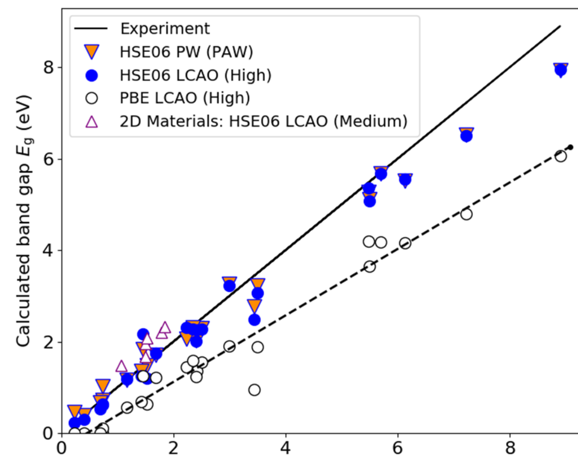

Fig. 1. Band gaps of 30 bulk materials and 2D (single monolayer) materials MoS_2, $MoSe_2$, $MoTe_2$, WS_2, WSe_2, BP. The LCAO/PW calculations are done with PD pseudopotential/PAW potential. All the 3D materials are listed in Table 3 in Ref. [9]. Experimental lattice parameters were used for all the calculations.

978-1-6654-0685-7/21/$31.00 ©2021 IEEE

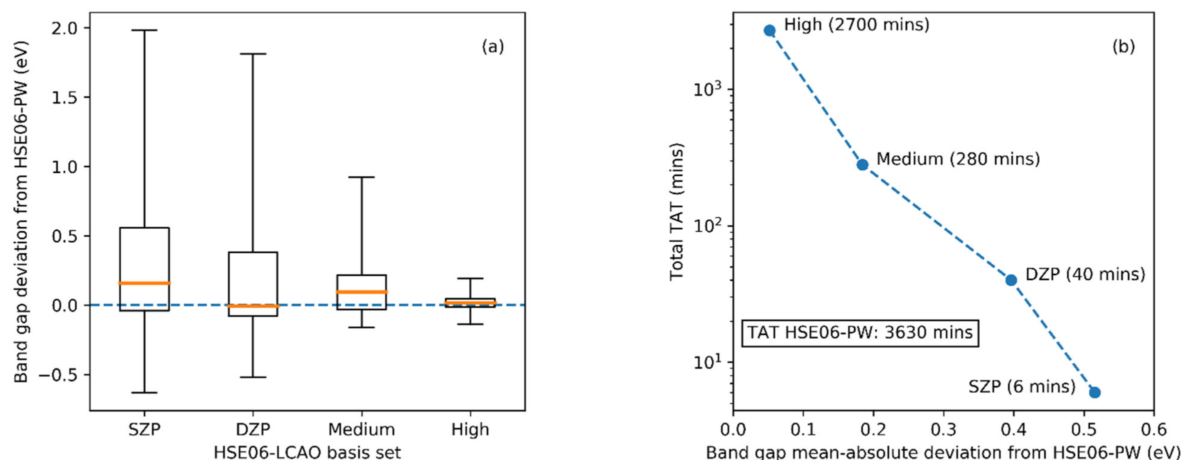

Fig. 2. Accuracy of HSE06-LCAO calculated band gaps (given in Fig. 1) for increasing LCAO basis-set size (in order SZP < DZP < Medium < and High), and total TAT for all 30 calculations for each basis set. **Left inset:** (a) Box-plot representations of deviations of HSE06-LCAO band gaps from reference HSE06-PW calculations. Each box extends from the lower (25%) to upper (75%) quantile of the distribution of band-gap deviations, with an orange solid line indicating the median. Whiskers indicate most-negative and most-positive values. **Right inset:** (b) TAT vs. QOR for each basis set (32 computing cores used). Note the y-axis log-scale. For comparison, the TAT for HSE06-PW using PAW potentials was 3630 min.

largely corrects for the band gap issue of local and semilocal functionals, such as PBE, and provides a better agreement with experimental results [10-14].

Figure 1 also includes band gaps of 2D materials calculated with HSE06-LCAO, which are all well described. A larger deviation from measured gaps might be attributed to excitonic effects [15] neglected in single-particle description of HSE06.

The HSE06-LCAO method significantly (up to 600x with SZP basis sets) reduces the computational turn-around time (TAT) as compared to the computationally demanding HSE06-PW approach, but larger basis sets may be needed for high-QOR results. We illustrate this in Fig. 2a, where HSE06-LCAO band gaps match HSE06-PW reference calculations increasingly well as the basis-set size increases. Figure 2b shows the trade-off between TAT and QOR; the TAT decreases 5-10x with each incremental reduction of basis-set size, which also increases the mean deviation from reference HSE06-PW calculations. However, the “Medium”-sized LCAO basis set provides an average QOR that is reasonably on par the PW method, while offering an order of magnitude lower TAT. Lastly, Figs. 2a and 2b indicate that for many gap materials, the Medium, DZP, or SZP basis sets may provide accurate band energies for HSE06-LCAO simulations with up to orders of magnitude TAT reductions, thereby enabling HSE06 simulations for systems comprising thousands of atoms on modest computational hardware.

B. Defect trap levels in bulk materials and interfaces

Material structures are rarely pristine, but often have a certain concentration of defects. Both native and intentional dopants play a key role, whether beneficial or detrimental, in a range of materials and devices [2,4,16]. Figure 3 clearly shows that having an accurate energy gap is important for QOR when calculating electronic trap levels in gap materials. HSE06-PW calculations allow for good QOR, but is computationally expensive for such defect simulations, which require large-scale atomistic modeling for a proper description

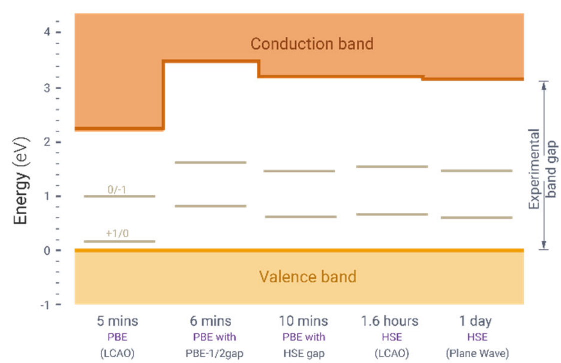

Fig. 3. Trap levels for Si vacancy in bulk 4H-SiC (128-atom supercell), calculated using full PBE, combined PBE-PBE-½, combined PBE-HSE06, full HSE06-LCAO, and full HSE06-PW approaches, all using PD/Medium pseudopotential/basis set, and run on 96 cores. The band gap obtained with HSE06-LCAO agrees well with the measured value [17].

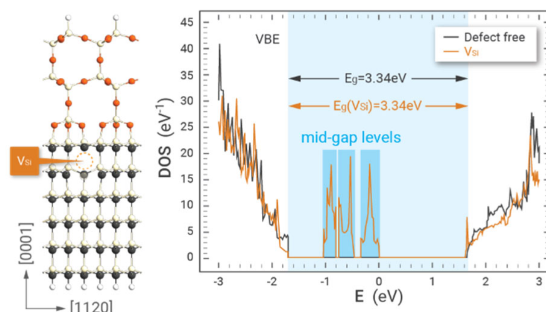

Fig. 4. Density-of-states for a 4H-SiC|SiO_2 interface with a Si vacancy (V_{Si}). Mid-gap levels appear between the Fermi level and the valance band edge (VBE). Simulations done with HSE-LCAO using FHI/DZP pseudopotential/basis set. The TAT was 28 min on 16 cores.

of charged defects. Using the HSE06-LCAO method eliminates this bottleneck, as suggested by the 15x lower TAT reported in Fig. 3 for simulations of charged defects in 4H-SiC, an important material within power electronics. The TAT can be further reduced by an order of magnitude if one adopts an approach where HSE06-LCAO provides a correction to the PBE band gap and band energy edges, see Fig. 3. We also

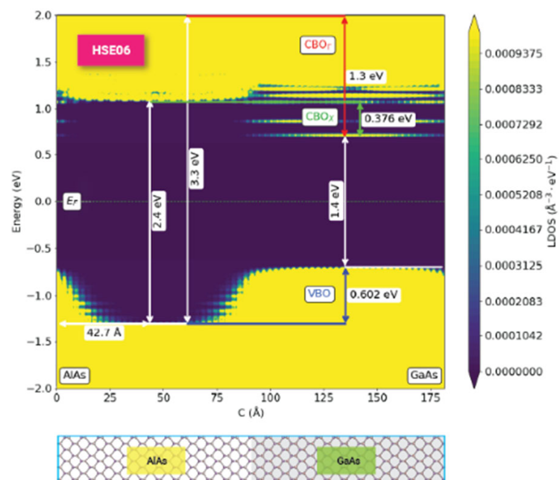

Fig. 5. Band diagram for a 128-atom AlAs|GaAs heterojunction obtained with HSE-LCAO using PD/Medium pseudopotential/basis set. The TAT was 98 min on 40 cores.

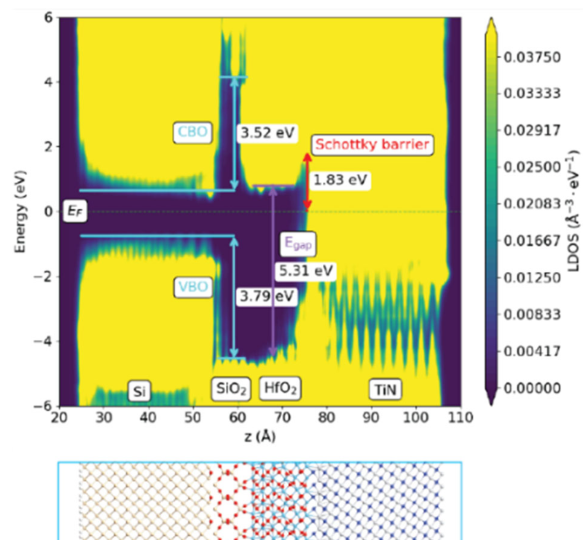

Fig. 6. HSE-LCAO obtained band diagram across a 748-atom $Si|SiO_2|HfO_2|TiN$ HKMG stack. The TAT was 9 hours using FHI/SZP pseudopotential/basis set. Increasing the system size to 2992 atoms by using 2x2 lateral unit cell (shown on the bottom) increases TAT to 45 hours only (on 40 cores).

demonstrate in Fig. 4 that HSE06-LCAO can be efficiently used for studying defect mid-gap levels at interfaces, here due to a Si vacancy at the $4H\text{-}SiC|SiO_2$ interface.

C. Heterojunction band alignment

Bringing two dissimilar semiconductors together to form an interface gives rise to a specific band alignment between these two materials, which depends on both bulk semiconductor properties (band gaps, affinities) and interface chemistry (contributing to interface dipole). The HSE06-LCAO method allows achieving accuracy for both bulk and interface properties with a moderate TAT. In Fig. 5, we report valence (VBO) and conduction (CBO) band offsets for the optoelectronics-relevant AlAs|GaAs heterojunction formed by III-V semiconductors (128 atoms). The calculated VBO of 0.60 eV agrees well with the measured VBO of 0.53 eV [18]. TAT for these HSE06-LCAO simulations of heterostructures varied within 19-98 minutes depending on the system size (48 – 128 atoms), suggesting nearly linear scaling, and that is at least an order of magnitude faster than what would typically be required with the HSE06-PW method. Note that reducing the system size would of course further reduce the TAT, but results would then suffer from finite-size effects. The HSE06-LCAO method avoids finite-size effects by enabling simulations for sufficiently large systems.

D. HKMG stack band diagram

The accuracy and efficiency of the HSE06-LCAO method for bulk materials and single interfaces suggest its suitability for studying complex material structures of industrial relevance, such as HKMG stacks with ultra-thin oxide layers used in logic technologies [19]. Figure 6 shows the band diagram across a $Si|SiO_2|HfO_2|TiN$ stack simulated using HSE06-LCAO. The band diagram allows calculating band energies, offsets and Schottky barriers at semiconductor-oxide, oxide-oxide and metal-oxide interfaces inside the stack. It also demonstrates band bending within semiconductor and oxide layers, and metal-induced states in high-k oxide. Even though the stack structure is comprised of 748 atoms, total TAT of the HSE06-LCAO calculations, using modest hardware resources, is 9 hours only, which is on par with that of standard PBE calculations.

Studying effects of HKMG defects or dopants at reasonable concentrations usually requires a larger gate-stack cross section. Increasing the system size to 2992 atoms (as seen at the bottom of Fig. 6) increases the TAT to 45 hours, again nearly linear scaling with respect to system size. We expect that HSE06-LCAO should also provide a reliable permittivity profile throughout the different HKMG stack layers, due to accurate band gaps and band energies of gap materials comprising the stack.

An important quantity characterizing gate stacks is the effective work function (EWF). This can be straightforwardly extracted from HSE06-LCAO simulations, as seen in Table 1, which shows that the HSE06-obtained EWF agrees well with measured data [19]. We note that atomistic modeling allows predicting trends in EWF shifts induced by interfacial dopants, e.g., *p*-type shift (an increase of EWF in Table 1) due to Al doping of the gate stack in Fig. 6.

Table 1. Effective work function for $Si|SiO_2|HfO_2|TiN$ HKMG stack w/wo Al dopants at $HfO_2|TiN$ inter-face. The EWF is calculated as $EWF = \Delta E_F + \chi$, where ΔE_F is the Fermi energy with respect to Si conduction band edge in the HKMG stack, obtained using the LDA or HSE06 approach, χ is the measured affinity of Si [19].

Al dopant concentration	Effective Work Function (eV)		
	LDA [19]	*HSE06-LCAO*	*Exp. [19]*
0	5.9-6.2	4.4	4.2-4.9
0.87 nm^{-2}	--	4.76	--
1.74 nm^{-2}		4.93	

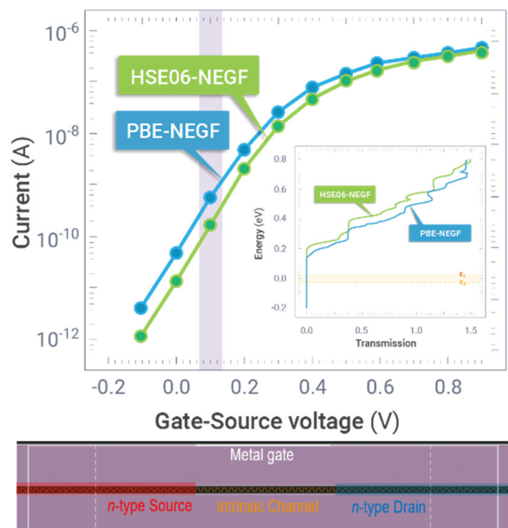

Fig. 7. IV characteristics and transmission spectrum for a BP-FET model device obtained with HSE06-NEGF and compared to PBE-NEGF. TAT=225 min (on 96 cores) using PD/Medium pseudopotential/basis set.

E. IV characteristics of 2D material-based FET

Ab initio device simulations under finite bias is a cornerstone of semiconductor electronic-structure modeling. The presented HSE06-LCAO method enables for the first-time atomistic modeling of microelectronic devices using hybrid DFT combined with the nonequilibrium Green's-function formalism (NEGF) for electron transport [9]. Using hybrid functionals for device simulations allows for proper description of electronic properties of all gap materials comprising the device on the same footing, without adjustable parameters. Figure 6 shows an example of how the accurate HSE06 description of electronic structure can affect simulated device characteristics for a black phosphorous (BP) based FET, as compared to standard PBE simulations. Note that PBE significantly (by more than 50%) underestimates the BP band gap, compared to experiment and HSE06 calculations. The increased band gap within HSE06-NEGF results in a reduced current for all gate-source voltages, and the subthreshold swing is reduced from 100 meV/dec (PBE-NEGF) to 90 meV/dec (HSE06-NEGF). The HSE06-NEGF methodology can equally well be applied to other 2D channel materials of industrial relevance, for instance, MoS_2 and WS_2 [20, 21].

IV. Conclusions

We implemented the HSE06 hybrid density functional using LCAO basis sets and norm-conserving pseudopotentials, enabling high QOR at reasonable TAT in *ab initio* simulations for semiconductor device technology development. The high QOR was confirmed by HSE06-LCAO simulations for a wide range of gap materials, interface and stack structures, suggesting up to orders of magnitude lower TAT than traditional implementations of HSE06, and almost linear scaling of TAT with respect to system size (number of atoms). Using HSE06-LCAO for NEGF-based electron transport simulations was shown to significantly impact device characteristics in a case where ordinary DFT is insufficient for accurate band energies. We expect this first-ever implementation of hybrid density functionals for device simulations in a commercial *ab initio* software package will allow for an improved description of device characteristics in atomistic modeling of future technology nodes. In summary, we believe that HSE06-LCAO will become a routine method of choice for applications that require both large-scale atomistic modeling and accurate electronic structure of gap materials.

V. References

[1] S.-K. Su, J. Cai, E. Chen, L.-J. Li, and H. -S. P. Wong, SISPAD 2020.
[2] G. Kang, J. Jeon, J. Kim, H. Ahn, I. Jang, D. Kim, SISPAD 2020.
[3] N. A. Lanzillo and R. R. Robison, 2019 IEEE Albany Nanotechnology Symposium.
[4] J. Wozny, A. Kovalchuk, J. Podgorski, and Z. Lisik, Materials 14, 1247 (2021).
[5] S. Yang, N. B. M. Schröter, V. N. Strocov, S. Schu-walow, M. Rajpalk et al., arXiv:2012.14935v1.
[6] J. Heyd, G. E. Scuseria, and M. Ernzerhof, J. Chem. Phys. 124, 219906 (2006).
[7] S. V. Levchenko, X. Ren, J. Wieferink, R. Johanni, P. Rinke, V. Blum, M. Scheffler, Comp. Phys. Comm. 192, 60 (2015).
[8] QuantumATK S-2021.06, https://www.synopsys.com/silicon/quantumatk.html
[9] S. Smidstrup, T. Markussen, P. Vancraeyveld, J. Wellendorff, J. Schneider, T. Gunst, B. Verstichel, et al., J. Phys.: Condes. Matter 32, 015901 (2020).
[10] J. Heyd, J. E. Peralta, G. E. Scuseria and R. L. Mar-tin, J. Chem. Phys. 123, 174101 (2005).
[11] M. Landmann, E. Rauls and W. G. Schmidt, J. Phys.: Condens. Matter 24, 195503 (2012).
[12] E. Bersch, S. Rangan, R. A. Bartynski, E. Garfunkel and E. Vescovo, Phys. Rev. B 78, 085114 (2008).
[13] L. I. Berger, CRC Handbook of Chemistry and Phys-ics 97th edn., Ed. J. R. Rumble (Boca Raton, FL: CRC Press) (2017).
[14] A. Ramasubramaniam, Phys. Rev. B 86, 115409 (2012).
[15] F. A. Rasmussen and K. S. Thygesen, J. Phys. Chem. C 119, 13169 (2015).
[16] Z. Wang, Z. Zhang, C. Shao, J. Robertson, S. Liu, and Y. Guo, IEEE Trans. Elec. Dev. 68, 288 (2021).
[17] Yu. Goldberg, M. E. Levinshtein, S. L. Rumyantsev, Advanced Semiconductor Materials GaN, AlN, SiC, BN, SiGe, Eds. M. E. Levinshtein, S. L. Rumyantsev, M. S. Shur (John Wiley & Sons, Inc., New York) (2001).
[18] I. Vurgaftman, J. Meyer, and L. Ram-Mohan, J. Appl. Phys. 89, 5815 (2021) (and references therein).
[19] P.-Y. Prodhomme, F. Fontaine-Vive, A. Van Der Geest, P. Blaise, and J. Even, Appl. Phys. Lett. 99, 022101 (2011).
[20] T. Agarwal et al., 2017 IEEE International Electron Devices Meeting (IEDM), 5.7.1-5.7.4 (2017).
[21] G. Arutchelvan, G, Q. Smets, Q., D. Verreck, et al, Sci. Rep. 11, 6610 (2021).